SENSITIVITY ANALYSIS OF HAPKE MODEL WITH LROC NAC – APPLICATION TO (DATA LIMITED) PLANETARY SURFACE CHARACTERIZATION IN THE OUTER SOLAR SYSTEM. V. Singh[1], A. R. Rhoden[2], H. Sato[3,4], M. S. Robinson[1,3], [1]SESE, Arizona State University, 781 Terrace Road, Tempe, AZ 85287 (Vishaal.Singh@asu.edu), [2]Southwest Research Institute, Boulder, CO, [3]LROC Science Operation Team, Arizona State University, Tempe, AZ, [4]Japan Aerospace Exploration Agency, Kanagawa, Japan.

Introduction: Planetary photometry is a useful tool for (near) surface characterization of distant bodies in the solar system – to infer physical properties (grain size, roughness, particle structure, compaction state) from the variation in intensity of reflected light as a function of illumination/viewing geometry. However, robust estimates of surface properties generally require observations over the broadest possible range of viewing & illumination angles [1]. This is particularly challenging for icy planetary surfaces, where we have limited observational data (eg: phase coverage). It is difficult to accurately determine viewing geometry, generate phase curves, fit models to data, and interpret the surface properties (through global & regional photometry).

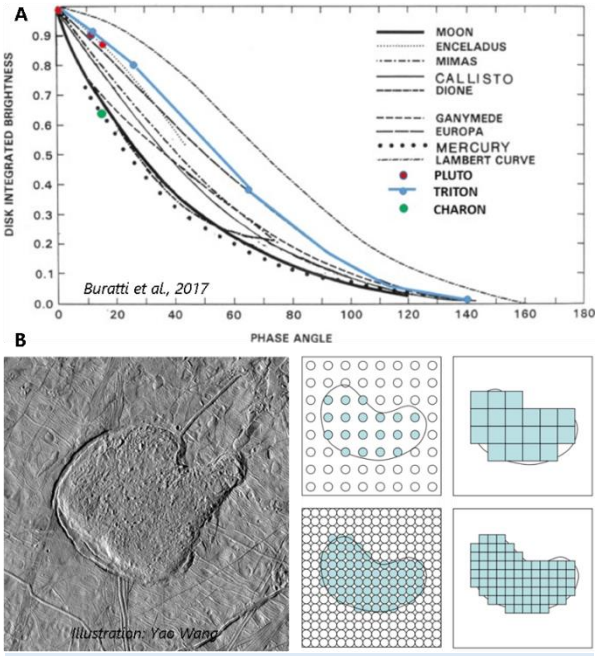

Fig 1. (A) Phase curves of outer solar system objects are difficult to generate due to relatively sparse data; (B) our sensitivity analysis will test whether surface properties of regional features (like chaos) can be accurately captured with limited datasets

The Hapke bidirectional reflectance model is the most widely used photometric model, utilizing radiative transfer methods to investigate the scattering properties of regoliths [2-3]. Its limitations are well documented, including application to well characterized lab samples, which reveal large inconsistencies in fitting parameters [4-6]. But there is still a need to determine the sensitivity of the model (*how do inferred parameters change?*) to datasets limited by parameters of (1) number of images, (2) image resolution, (3) phase coverage, and (4) topography (see Fig. 1). We have developed an iterative approach to address this knowledge gap, starting with lunar datasets to benchmark our results.

Why start with the Moon?: Over the past decade, the Lunar Reconnaissance Orbiter Camera (LROC) has provided >500,000 multispectral observations of the Moon, including extensive regional coverage under various illumination conditions with unparalleled image resolution (down to 0.5 m-scale). This rich dataset not only provides a near comprehensive spectral-photometric picture of the Moon, but also allows us to test model sensitivity across the range of observations potentially available for outer solar system bodies.

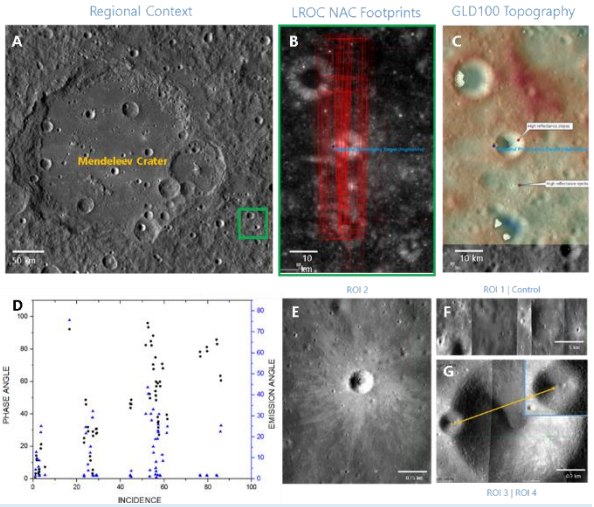

Fig 2.(E-G) Selected region lies next to Mendeleev Crater (A), with (B,D) 70 NAC observations spanning broad range of illumination/viewing geometry & (C) DTM coverage

Methodology: Sato et al. 2014 [7] used 66,00 LROC Wide Angle Camera (WAC) images to derive near-global Hapke parameter maps (1°x1° grid) of the Moon – this establishes a (global) baseline for comparison with our regional photometry.

Site Selection: Our region of interest was chosen in the (higher albedo) highland terrain close to Mendeleev Crater (5.7°N 140.9°E). We selected [i] a relatively homogeneous control region, [ii,iii] two young craters (D = 0.25 km & 1 km), and [iv] a region with fresh, immature ejecta near a young crater (see Fig. 2A, E-G).

Dataset: We utilized a multispectral multitemporal LROC Narrow Angle Camera (NAC) dataset of 70

images acquired from August 2010 to November 2016, with incidence=1°-86°, emission=1°-75°, phase=0.5°-86° coverage (Fig 2B-C). The raw image data is archived in NASA Planetary Data System (PDS) Experiment Data Record (EDR) format.

Image Processing: Multiple NAC images for each region were acquired, radiometrically calibrated & photometrically normalized to a common viewing geometry and illumination angle, following the procedure described in [7]. The geographic location (latitude, longitude), incidence, emission and phase angles of each image pixel were accurately computed using LRO-derived Camera Kernels, and GLD100 Digital Terrain Model (100 m/pixel) [8].

Phase Curve & Model Fitting: Phase curves were generated for each region using the repeat NAC image coverage, with a sampling box used to constrain image footprints within the region. Using the Hapke parameter calculation procedure developed by [7], we simplified the model using empirical relations & parameter assumptions. Also, we ensured a consistent range of i,e,g for all sampling sites to avoid dependence of fitting on range at this stage. We derive three spatially resolved Hapke parameters (*single scattering albedo w, phase function parameter b, and angular width of shadow hiding opposition effect (SHOE)* h_S). These derived parameters serve as our regional baseline for comparison.

Parameters Investigated: To test the model sensitivity, we modify the available 'inputs' for each region over multiple iterations and determine the regional properties. In each case, these properties are statistically compared to both global & regional baselines (using a two sample Kolmogorov–Smirnov test). This allows us to identify whether the derived parameters are still representative of the sampled region, and eventually determine the threshold where they are not.

We will discuss the results of multiple tests:

Number of Images: In preliminary work, we reduced the number of images available for all the selected regions (by half), and generated phase curves (Fig. 3). The young crater and ejecta blanket both show distinct curves, particularly at high phase angles, potentially due to loss of phase coverage in remnant dataset. We are currently determining Hapke parameters, but expect them to be similarly distinct.

Image Resolution: We (stepwise) reduce the resolution of NAC images lying within the sampling box (eg: using mean filtering of image pixel DN values) to gauge if large image footprints of lower resolution (km scale) can still capture small scale surface properties.

Phase Coverage: We are primarily focusing on the influence of phase angles between 0°-5°and >75°, to capture the 'opposition surge' effect, which influences the amplitude & angular width of the SHOE and Coherent Backscatter (CBOE) Hapke parameters.

Topography: Current work uses [i] a shape model and [ii] GLD100 DTM respectively for calculation of illumination conditions. In future, we plan to use NAC DTMs (~50m/pixel) to further refine this calculation.

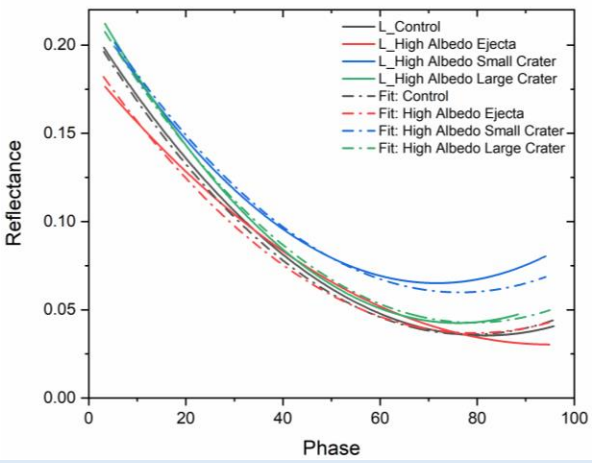

Fig 3. Reduced image footprints led to distinct phase curves for selected regions – prominently in 0.25-0.5 km size range

Future Work & Implications: The interpretation of Hapke photometric properties for planetary surfaces needs to be pursued with caution. We will combine our ongoing sensitivity analysis with [i] pre-existing estimates of lunar surface properties, and [ii] measured properties of lunar return samples to benchmark our results with 'ground truth'. This will allow us to deliver the minimum spatial resolution, phase coverage, and number of observations needed by the Hapke model to differentiate between nearby surface terrains. It can also help identify uncertainties in adaptation for icy satellite datasets & conditions, and serve as a guideline for interpreting future mission datasets.

In future, we plan to validate these results by extending this analysis to the Pluto-Charon system with New Horizons datasets and Jovian system with Galileo (and future Europa Clipper).

Acknowledgments: We acknowledge the LROC team for providing access to the NAC image dataset and selection of region of interest for this analysis.

References: [1] Verbiscer et al. (2013) Astrophysics and Space Science Library 356; [2] Hapke, B. et al. (1981) JGR, 86, 3055–3060; [3] Hapke, B. et al. (2012) Icarus, 221, 1079–108; [4] Shepard, M. and Helfenstein, (2007) JGR, 112, E3. [5] Shkuratov, Y. et al. (2007) JQSRT, 106, 487–508; [6] Pilorget, C. et al. (2016) Icarus, 267, 296–314; [7] Sato, H. et al. (2014) JGR- Planets, 119, 1775–1805; [8] Scholten et al. (2012) JGR, 117, E00H17.